CONSTRICTION RESISTANCE OF PLANAR ISOFLUX HEAT SOURCES WITHIN SEMI-INFINITE CONDUCTORS: IMAGE METHOD

M.M.Yovanovich
Professor and Director, Fellow ASME
Microelectronics Heat Transfer Laboratory
Department of Mechanical Engineering
University of Waterloo
Waterloo, Ontario, Canada N2L 3G1

ABSTRACT

A novel procedure is presented for determining thermal constriction resistances of planar isoflux heat sources of arbitrary shape which are located at arbitrary depths below the interface formed by two solids of different, but isotropic, thermal conductivities. The procedure is applied to circular annular heat sources which includes the circle as a limiting case. Dimensionless constriction resistances are shown to be functions of three dimensionless parameters which are: the annular radii ratio, ii) the relative depth, and iii) the thermal conductivity ratio. The constriction resistance is the sum of the self-effect which has analytic solutions and the effect of the image which requires numerical integration. Numerical results are presented in graphical and tabular form. Correlation equations are provided for easy use by designers of microelectronic and telecommunication devices and components.

NOMENCLATURE

A	=	heat source area; m^2
a, b	=	inner and outer radii of annulus; m
$C_1, C_2,$ C_3, C_4	=	correlation coefficients
c	=	distance of planar source from interface; m
$E(\epsilon)$	=	complete elliptic integral of the second kind
G_s, G_i	=	geometric parameter
$K(\epsilon)$	=	complete elliptic integral of the first kind
Q	=	total heat flow rate; W
q	=	heat flux; W/m^2
R	=	thermal resistance; K/W
$R^*_{\sqrt{A_p}}$	=	dimensionless thermal resistance
r_1, r_2	=	distances from source and image to field point; m
s_1, s_2	=	source and image strengths; W
T_1, T_2	=	temperatures in medium 1 and 2; K
$\overline{T}$	=	area average temperature; K
x, y, z	=	cartesian coordinates; m

Subscripts

A_p	=	based on A_p as the characteristic length
0	=	at the centroid
i	=	due to the image
s	=	due to the source

Greek Symbols

γ	=	relative depth; $\gamma = c/b$
ϵ	=	radii ratio; $\epsilon = a/b$
η	=	conductivity parameter, $\eta = (1-\kappa)/(1+\kappa)$
κ	=	conductivity ratio λ_1/λ_2
λ_1, λ_2	=	conductivities of materials; $W/m \cdot K$
ρ, θ	=	polar coordinates

INTRODUCTION

The steady-state thermal resistance of heat sources which are located a certain distance from a plane interface formed by two different solids is currently of some interest within the microelectronics and telecommunication industries. Since the heat sources are sufficiently thin with respect to the other dimensions, therefore they can be modeled as planar heat sources with uniform heat flux.

Since the dimensions of the contacting solids are orders of magnitude larger than the largest dimension of the heat source, therefore the solids can be modeled as half-spaces.

The interface has very good thermal contact; therefore it is taken to be in perfect contact. Further the contacting solids may have similar or significantly different thermal conductivities.

Conventional solution methods are very difficult or impossible to apply to this class of thermal problems. Numerical methods can be applied, but they are computationally intensive and the industries prefer simpler, less computationally intensive methods.

In electrostatics there is a class of electrical problems which are mathematically identical to the above thermal problems, and they are solved by the method of images. Although this method has been applied to find electrical fields and it is well-established (Kellogg, 1953, Jeans, 1963, and Lorrain and Corson, 1970), it seems that it has not been used to find temperature fields and thermal constriction resistances which are currently of great interest to designers of microelectronic and telecommunication devices and components.

The objective of this paper is to present a procedure based on the method of images to determine thermal constriction resistances of planar isoflux heat sources of arbitrary shape which are embedded in an isotropic solid which is in perfect contact with another solid which is denoted as the substrate.

The proposed method will be applied to circular annular heat sources (which will be referred to as contacts) to demonstrate its ease of application and its usefulness.

METHOD OF IMAGES

The method of thermal images will be applied to the determination of temperature distributions produced by a point thermal source situated in a material having thermal conductivity λ_1. The heat source of strength s is located a distance c from the plane interface which separates two media having thermal conductivities λ_1 and λ_2 respectively as shown in Fig. 1. Polar coordinates are used in the analysis.

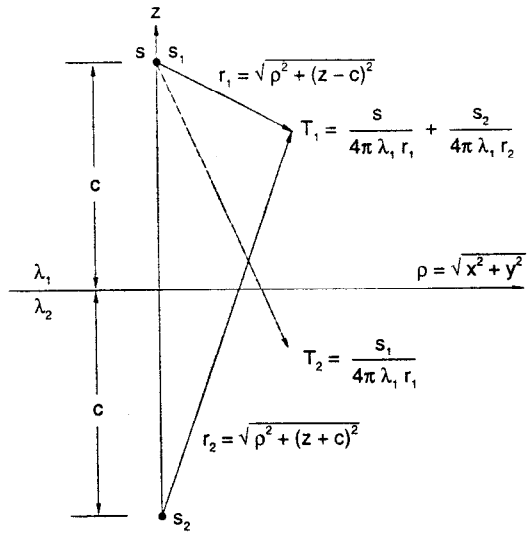

Fig. 1 Source and images and co-ordinate system.

We begin the analysis by considering the temperature distribution produced by a single thermal source of strength $s = qdA$ where q is the local heat flux and dA is the local elemental source area. The image of the heat source s_2 is located on the axis passing through the point source, a distance c below the common interface. The presence of s_2 in the material of conductivity λ_2 requires an image s_1 located at the source within the solid of conductivity λ_1.

The temperature distribution within the solid $z \geq 0$ is obtained by the linear superposition of the temperature fields produced by the source s itself and its image s_2

$$T_1 = \frac{s}{4\pi\lambda_1 r_1} + \frac{s_2}{4\pi\lambda_1 r_2} \tag{1}$$

where the distances from the source and its image are $r_1 = \sqrt{\rho^2 + (z-c)^2}$ and $r_2 = \sqrt{\rho^2 + (z+c)^2}$ respectively, and $\rho^2 = x^2 + y^2$.

The temperature distribution within the solid $z \leq 0$ of conductivity λ_2 is produced by the image s_1 which is at the distance r_1 and it is assumed that the entire system has conductivity λ_1 as shown in Fig. 1. The temperature field is given by

$$T_2 = \frac{s_1}{4\pi\lambda_1 r_1} \tag{2}$$

The strengths of the two images s_1 and s_2 respectively can be obtained from the application of the *perfect* contact conditions at the common interface $z = 0$. These conditions are

$$T_1 = T_2 \tag{3}$$

and

$$\lambda_1 \frac{\partial T_1}{\partial z} = \lambda_2 \frac{\partial T_2}{\partial z} \tag{4}$$

The temperature equality condition requires that

$$s + s_2 = s_1 \tag{5}$$

and the normal heat flux equality condition requires that

$$\lambda_1 \frac{\partial}{\partial z}\left(\frac{1}{r_1}\right) + \lambda_1 \frac{\partial}{\partial z}\left(\frac{1}{r_2}\right) = \lambda_2 \frac{\partial}{\partial z}\left(\frac{1}{r_1}\right) \tag{6}$$

which gives

$$\lambda_1 \left[\frac{-cs + cs_2}{(\rho^2 + c^2)^{3/2}}\right] = \lambda_2 \left[\frac{-cs_1}{(\rho^2 + c^2)^{3/2}}\right] \tag{7}$$

From Eq. (7) we find

$$-\lambda_1 s + \lambda_1 s_2 = -\lambda_2 s_1 \tag{8}$$

The image strengths are obtained from the solutions of Eqs. (5) and (8):

$$s_1 = \frac{2\lambda_1}{\lambda_1 + \lambda_2} s \qquad \textit{and} \qquad s_2 = -\left[\frac{\lambda_2 - \lambda_1}{\lambda_2 + \lambda_1}\right] s \tag{9}$$

After finding the image source strengths the temperature distributions within the two solids can now be written as

$$T_1 = \frac{s}{4\pi\lambda_1 r_1} - \left[\frac{\lambda_2 - \lambda_1}{\lambda_2 + \lambda_1}\right] \frac{s}{4\pi\lambda_1 r_2} \qquad z \geq 0 \tag{10}$$

and

$$T_2 = \left[\frac{2\lambda_1}{\lambda_1 + \lambda_2}\right] \frac{s}{4\pi\lambda_1 r_1} \qquad z \leq 0 \tag{11}$$

Limiting Cases

The limiting cases of T_1 can be deduced by examination of the second term of Eq. (10). If $\lambda_2 > \lambda_1$, the term is negative and it (image) behaves like a thermal sink. On the other hand if $\lambda_2 < \lambda_1$, the term is positive and it (image) behaves like a thermal source.

If $\lambda_2 >> \lambda_1$, the interface is isothermal ($T = 0$), and when $\lambda_2 << \lambda_1$, the interface is adiabatic.

Therefore the general solution, Eq. (10), yields two limiting cases of a point heat source located a distance c from 1) an isothermal plane and 2) an adiabatic plane, respectively.

PLANAR HEAT SOURCES–INTEGRAL SOLUTION

The fundamental solutions developed in the preceding section can be used to develop temperature fields produced by distributed planar heat sources which are positioned a fixed distance below the plane interface formed by two isotropic media having conductivities λ_1 and λ_2 respectively.

Consider a planar heat source of active planar area A_1 located a distance c from the interface $z = 0$ which separates two semi-infinite media having conductivities λ_1 and λ_2 as shown in Fig. 2.

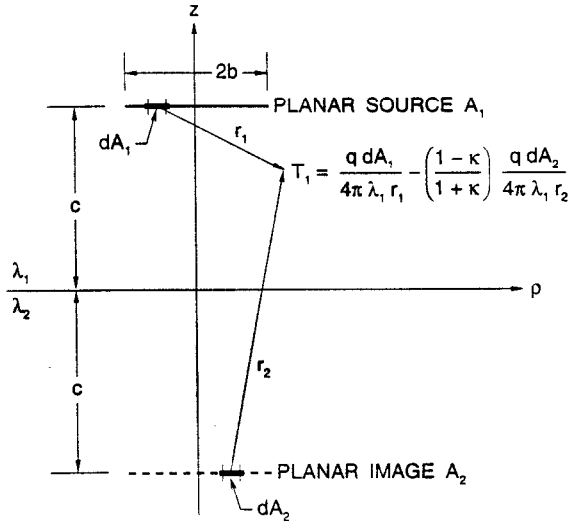

Fig. 2 Planar source and its image.

The heat flux q over the heat source is assumed to be uniform. The image of the heat source having surface area A_2 is shown as a broken line in the material λ_2. Its heat flux q_2 is also taken to be uniform.

The temperature distribution at an arbitrary field point within material λ_1 produced by arbitrary point heat sources lying within areas A_1 and A_2 is obtained by means of the fundamental solution given above:

$$T_1 = \frac{q dA_1}{4\pi\lambda_1 r_1} - \eta \frac{q dA_2}{4\pi\lambda_1 r_2} \tag{12}$$

and after integration over the heat source area and its image area we obtain the temperature distribution at any field point to be

$$T_1 = \frac{q}{4\pi\lambda_1}\left[\int\int_{A_1} \frac{dA_1}{r_1} - \eta \int\int_{A_2} \frac{dA_2}{r_2}\right] \tag{13}$$

where the thermal parameters are defined as

$$\eta = \frac{1 - \kappa}{1 + \kappa} \qquad \text{and} \qquad \kappa = \frac{\lambda_1}{\lambda_2} \tag{14}$$

Both sides of the heat source and its image must be included in the integrations of Eq. (13). The basic solution, Eq. (13), can be used to determine the local

and area-average temperatures of the planar heat source of any shape.

AVERAGE SOURCE TEMPERATURE AND CONSTRICTION RESISTANCE

Average Source Temperature

For applications of the fundamental solutions given above it is necessary to define the average source temperature as

$$\overline{T}_1 = \frac{1}{A_1}\int\int_{A_1} T_1 dA_1 \tag{15}$$

After substitution of Eq. (13) with Eq. (14) into the above definition we obtain the area-average temperature of the isoflux heat source:

$$\overline{T}_1 = \frac{q}{4\pi\lambda_1}\frac{1}{A_1}\int\int_{A_1}\left\{\int\int_{A_1}\frac{dA_1}{r_1} - \eta\int\int_{A_2}\frac{dA_2}{r_2}\right\}dA_1 \tag{16}$$

Constriction Resistance

The constriction (or spreading) resistance (Yovanovich, 1976a) is a useful concept for providing means of simple analysis. It is defined as the average temperature of the heat source minus the average temperature of the heat sink (which is taken to be zero) divided by the total heat transfer rate from the source. Therefore

$$R = \frac{\overline{T}_1}{Q_1} = \frac{\overline{T}_1}{qA_1} \tag{17}$$

which yields

$$R = \frac{1}{4\pi\lambda_1}\frac{1}{A_1^2}\int\int_{A_1}\left\{\int\int_{A_1}\frac{dA_1}{r_1} - \eta\int\int_{A_2}\frac{dA_2}{r_2}\right\}dA_1 \tag{18}$$

The above result can be applied to any singly-connected or doubly-connected planar heat source geometries. The first term represents the *self-effect* of the heat source and the second term accounts for the effect of the image on the source temperature.

The previous expression will be nondimensionalized with respect to the thermal conductivity of the solid in which the heat source is embedded λ_1. The square root of the projected area is chosen as the characteristic length $\sqrt{A_p}$ (Yovanovich and Burde, 1977).

The dimensionless constriction resistance can be written simply as

$$R^*_{\sqrt{A_p}} = G_s - \eta G_i \tag{19}$$

where G_s is a geometric parameter which represents the self-effect of the source, and G_i is a geometric parameter which represents the effect of the image on the source.

The first geometric parameter can be derived directly from the analytic expression developed for constriction resistances of isoflux annular contact areas situated on the surface of insulated half-spaces. Using the result of Yovanovich and Schneider (1976b) which was obtained by means of the integral formulation of Yovanovich (1977) and taking into account the differences between full-space and half-space solutions one obtains:

$$G_s = \left(\frac{4}{3\pi^{3/2}}\right)\frac{1}{(1-\epsilon^2)^{3/2}}\left[1+\epsilon^3-(1+\epsilon^2)E(\epsilon) + (1-\epsilon^2)K(\epsilon)\right] \tag{20}$$

where $K(\epsilon)$ and $E(\epsilon)$ are the complete elliptic integrals of the first and second kinds respectively. They are computed quickly and accurately by *Mathematica* (Wolfram, 1991) or any other Computer Algebra System.

This parameter has the value 0.23945 for the circular source $\epsilon = 0$, and it varies slowly in the range $0 \le \epsilon < 0.7$.

The parameter which accounts for the effect of the image on the source does not have an analytic solution. Numerical integration methods were used to obtain accurate values for several values of the independent parameters ϵ and γ which is the relative depth parameter. The numerical results were correlated accurately by means of the following simple poylnomial:

$$G_i = \frac{C_1}{C_2+\gamma} + \frac{C_3}{(C_4+\gamma)^2} \tag{21}$$

The correlation coefficients C_1 through C_4 for selected values of the parameter ϵ are given in Table 1. The maximum difference between the correlation and the numerical results is 0.76 % which occurs at $\epsilon = 0.7$.

Table 1: Correlation Coefficients for Geometric Effect of the Image

ϵ	C_1	C_2	C_3	C_4	% diff.
0.0	.0754568	2.5773	.141128	.81999	0.22
0.1	.0692988	1.9399	.127318	.79615	0.40
0.3	.0565473	.40206	.064440	.93120	0.34
0.5	.0371546	.29559	.112403	1.4833	0.58
0.7	.0141819	.18178	.159437	1.8690	0.76

NUMERICAL RESULTS AND DISCUSSION

The numerical results are presented in Figures 3 through 7 for several circular annular sources. The dimensionless constriction resistances are plotted against the thermal conductivity parameter η for the full range $-1 \le \eta \le 1$, and the relative source depth range $0 \le \gamma < \infty$.

Figure 3 shows the results for a circular heat source $\epsilon = 0$. The horizontal line at $R^*_{\sqrt{A_p}} = 0.23945$ represents the case where the source is embedded deep inside the solid and the effect of the substrate conductivity is negligible. Results to the left of $\eta = 0$ pertain to a substrate whose conductivity is less than that of the solid in which the source is embedded. This is the *resistive* portion of the solution and the dimensionless resistances are seen to be greater than the isolated source value. At $\eta = -1$ the interface is adiabatic.

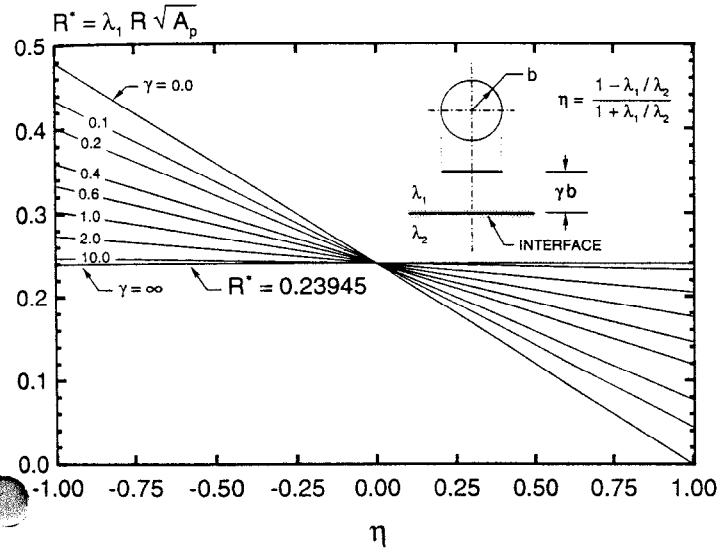

Fig. 3 Constriction resistance of circular heat source.

Results to the right of $\eta = 0$ correspond to a substrate whose thermal conductivity is greater than the conductivity of the solid. This is the *conductive* portion of the solution and the dimensionless constriction resistance is seen to be lower than the isolated source value. At $\eta = 1$ the interface is at the sink temperature which was set to zero in this analysis.

Figures 4 through 7 show the dimensionless constriction resistance plotted against η for selected values of γ and ϵ. Each figure corresponds to a different value of ϵ. These figures show the slow change in the dimensionless constriction resistance as ϵ varies.

CONCLUDING REMARKS

The method of images has been used to develop solutions of the Laplace equation for planar isoflux heat sources of arbitrary shape. The solutions in the form of temperature distributions at arbitrary field points are used to determine the dimensionless constriction resistance of arbitrary planar heat sources which are placed at arbitrary points below an interface separating the solid in which the heat source is embedded and the substrate.

The general expressed is used to derive the solution for a circular annular heat source. The solution was expressed in terms of two geometric parameters pertaining to the self-effect of the source and the effect of the image on the source. The geometric parameter for the image depends on the size of the circular annular area and its relative depth. A correlation equation was presented for accurate calculation of the image parameter G_i.

Numerical results for the circular and annular sources were presented for a selected range of the pertinent geometric and thermal parameters.

ACKNOWLEDGMENTS

The author acknowledges the financial support of the Natural Sciences and Engineering Research Council of Canada under operating grant A7455. The assistance of K. Martin in the computations of the data is greatly appreciated. Also the help of P. Teertstra and M. R. Sridhar in the preparation of the figures, plots and text is greatly appreciated.

REFERENCES

Jeans, J., 1963, *The Mathematical Theory of Electricity and Magnetism*, Fifth Edition, Cambridge University Press, pp. 200-201.

Kellogg, O.D., 1953, *Foundations of Potential Theory*, Dover Publications, New York, pp. 206-211.

Lorrain, P., and Corson, D.R., 1970, *Electromagnetic Fields and Waves*, Second Edition, W.H. Freeman and Company, San Francisco, pp. 153-156.

Wolfram, S., 1991, *Mathematica, A System for Doing Mathematics by Computer*, Second Edition, Addison-Wesley Publishing, Redwood City, CA.

Yovanovich, M.M., 1976a, "Thermal Constriction Resistance of Contacts on a Half-Space: Integral Formulation," ed. A.M. Smith, *Radiative Transfer and Thermal Control*, Progress in Astronautics and Aeronautics, Vol. 49, pp. 397-418.

Yovanovich, M.M., and Schneider, G.E., 1976b, "Thermal Constriction Resistance Due to a Circular Annular Contact," ed. A.M. Smith, *Thermophysics of Spacecraft and Outer Planet Probes*, Vol. 56, pp. 141-154.

Yovanovich, M.M., and Burde, S.S., 1977, "Centroidal and Area Average Resistances of Nonsymmetric, Singly Connected Contacts," *AIAA Journal*, Vol. 15, No. 10. October, pp. 1523-1525.

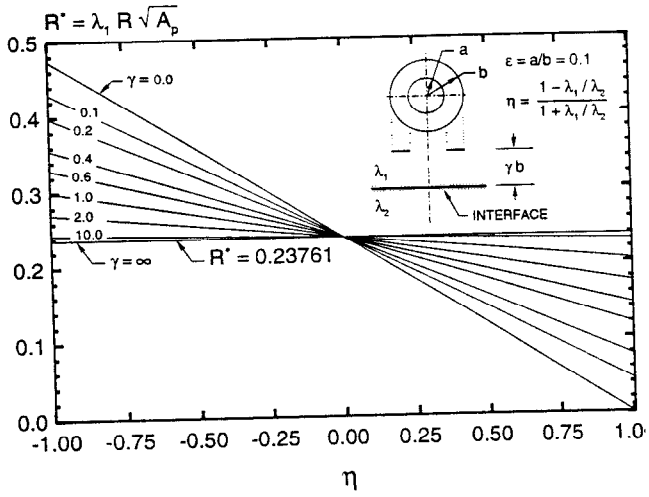

Fig. 4 Constriction resistance of annular heat source, $\epsilon = 0.1$.

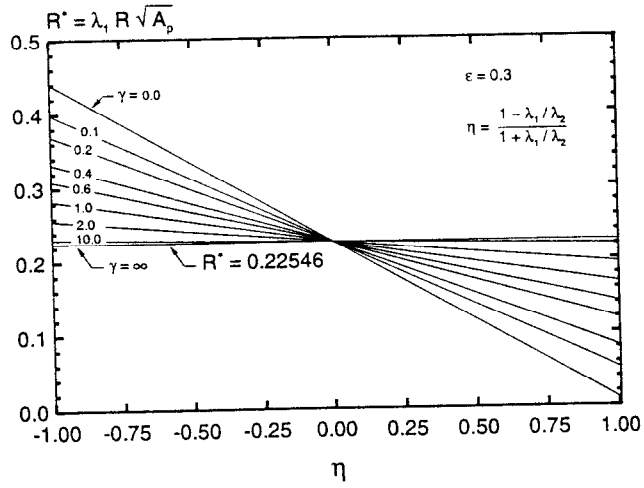

Fig. 5 Constriction resistance of annular heat source, $\epsilon = 0.3$.

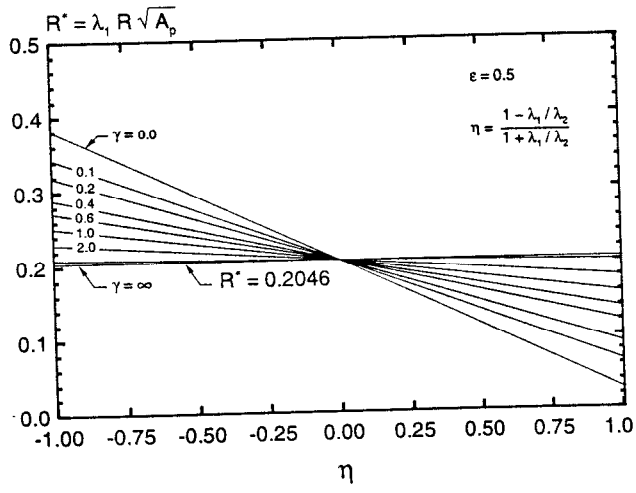

Fig. 6 Constriction resistance of annular heat source, $\epsilon = 0.5$.

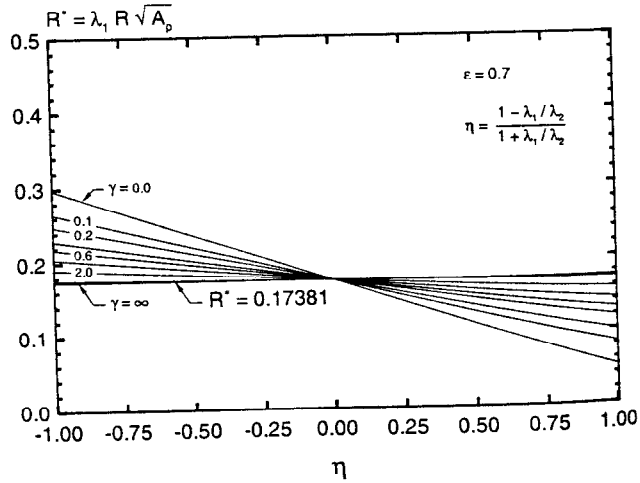

Fig. 7 Constriction resistance of annular heat source, $\epsilon = 0.7$.